

Fourier Methods for Kinematic Synthesis of Coupled Serial Chain Mechanisms

Xichun Nie

Department of Mechanical Engineering,
Center for Intelligent Machines,
McGill University,
3480 University Street, No. 421,
Montreal, Quebec, Canada
email: xichun_nie@hotmail.com

Venkat Krovi

Department of Mechanical and Aerospace
Engineering,
State University of New York at Buffalo,
318 Jarvis Hall,
Buffalo, NY
email: vkrovi@eng.buffalo.edu

Single degree-of-freedom coupled serial chain (SDCSC) mechanisms are a class of mechanisms that can be realized by coupling successive joint rotations of a serial chain linkage, by way of gears or cable-pulley drives. Such mechanisms combine the benefits of single degree-of-freedom design and control with the anthropomorphic workspace of serial chains. Our interest is in creating articulated manipulation-assistive aids based on the SDCSC configuration to work passively in cooperation with the human operator or to serve as a low-cost automation solution. However, as single-degree-of-freedom systems, such SDCSC-configuration manipulators need to be designed specific to a given task. In this paper, we investigate the development of a synthesis scheme, leveraging tools from Fourier analysis and optimization, to permit the end-effectors of such manipulators to closely approximate desired closed planar paths. In particular, we note that the forward kinematics equations take the form of a finite trigonometric series in terms of the input crank rotations. The proposed Fourier-based synthesis method exploits this special structure to achieve the combined number and dimensional synthesis of SDCSC-configuration manipulators for closed-loop planar path-following tasks. Representative examples illustrate the application of this method for tracing candidate square and rectangular paths. Emphasis is also placed on conversion of computational results into physically realizable mechanism designs. [DOI: 10.1115/1.1829726]

1 Introduction

Coupled serial chains are a novel mechanism configuration formed by coupling the distal joint rotations of multilink serial chain to their proximal joint rotations, using either gears or cable-pulley drives [1]. Each physical coupling reduces a degree-of-freedom and repeated couplings progressively reduce the overall degrees of freedom to one. The resulting single degree-of-freedom coupled serial chain (SDCSC) mechanism, shown in Fig. 1(a) requires only a single actuator at the base to drive the entire system.

Such SDCSC mechanisms can be used to realize a broad range of end-effector trajectories using just single degree-of-freedom actuation. Trajectories of increasing complexity and variety may be generated by increasing the number of links of the SDCSC mechanism, as illustrated in Fig. 1(b). As Hunt [2], notes, "there is no limit to the possible arrangements when gears and bands are used especially for noncircular gears or band wrapping profiles." The principal benefits of such SDCSC mechanisms ensue from their ability to combine the simplicity of single-degree-of-freedom control and rigidity/strength, of the type afforded by closed-loop linkages, with the modularity, compactness, and reduced interference of serial chains.

Articulated manipulation-assistive aids, that can interact with and augment the manipulation skills of humans, have applications in diverse arenas from manufacturing assembly lines to rehabilitation engineering. However, most general-purpose manipulator designs possess multiple degrees-of-freedom within the chain, which are often excessive for performing typical low-dimensional manipulation tasks. Such excessive degrees of freedom then need to be reduced by application of constraints, either *passively using hardware-constraints* or *actively by suitable control*, prior to performance of the task.

Our interest, therefore, is on creating articulated manipulation-assistive aids based on the SDCSC configuration that can work passively in cooperation with the human operator or to serve as a low-cost automation solution. Figure 2 depicts a potential industrial application of such an SDCSC-configuration manipulation-assistive device [3,4]. The end-effector forms a passive virtual guide rail to constrain the motions of the user to the prescribed task-space curve. The selection of the SDCSC configuration helps combine the motion flexibility due to the multiple articulations with the simplicity of reduced degree-of-freedom control due to the presence of hardware constraints. Additionally, the hardware-based constraint implementation also offers improved reliability, excellent repeatability, passivity/stability of the constraint implementation and low development and maintenance costs when compared to active software-control based constraint implementations. Such SDCSC-based manipulators offer significant potential for application as a low-cost and passive alternative to actively coordinated robotic manipulators for many typical industrial automation tasks.

However, such manipulators need to be synthesized specifically for desired tasks. In this paper, we focus our attention on development of tools from Fourier analysis and optimization to permit the end effectors of such SDCSC-type manipulators to trace desired closed paths in the plane. The organization of the rest of this paper is as follows: Section 2 surveys some of the related background on similar mechanism configurations and design/synthesis methods reported in the literature. Section 3 briefly provides the required mathematical background for the developments in this paper. Section 4 discusses the applicability of traditional mechanism synthesis methods before presenting the proposed Fourier-based synthesis method and discussing its nuances. The application of this method to the design of SDCSC-type manipulators to trace square and rectangular paths is presented in Sec. 5. Section 6 discusses the process of conversion of these mathematical results into physically realizable designs and Sec. 7 concludes this paper.

Contributed by the Mechanisms and Robotics Committee for publication in the JOURNAL OF MECHANICAL DESIGN. Manuscript received December 5, 2003; revised June 2, 2004. Associate Editor: Q. J. Ge.

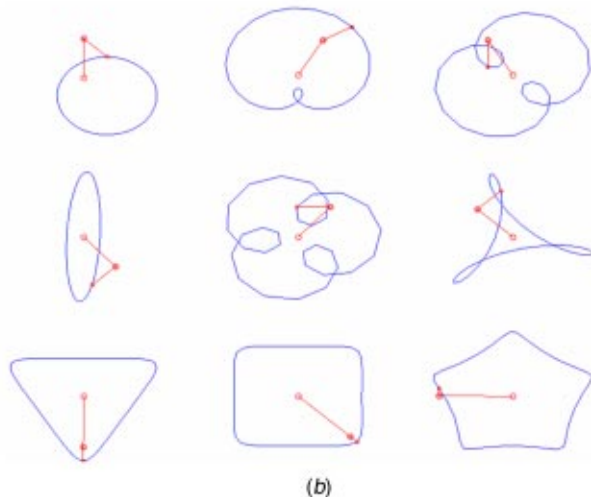
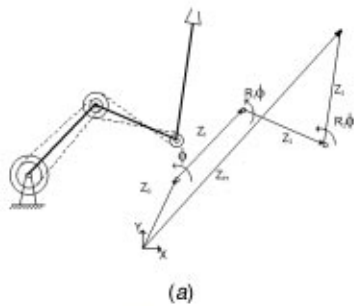


Fig. 1 (a) Three-link single degree-of-freedom coupled serial chain (SDCSC) mechanism; (b) typical end-effector paths of SDCSC mechanisms

2 Literature

The characteristic feature of SDCSC mechanisms is the direct coupling of joint rotations within the mechanism using *hardware* constraints. Inasmuch, such mechanisms share many features in common with *geared* and *tendon-driven mechanisms* which we will briefly survey (but with our attention focused on implementations with linear coupling of joint rotations).

The use of gear pairs to couple joint rotations has been studied in the literature principally in the context of closed-loop geared mechanisms. The cycloid crank was developed as an extension of the $R-R$ crank by replacing the revolute joints with gear pairs. Sandor [5] developed the “Cycloidal Burmester Theory” for use in the synthesis of cycloid cranks to reach the maximum number of precision points. Wunderlich [6] presented a detailed *analysis* of “higher cycloids” created by substituting gear pairs for revolute joints in long articulated chains. However, further extensions to the cycloidal Burmester theory for synthesis of longer coupled chains were never pursued with the notable exception of the Bicycloidal crank [7].

Most literature on tendon-driven mechanisms focuses on the full control of an n -dof manipulator (see Tsai [8] for a good review). Fewer examples of use of tendon-driven actuation to reduce the degrees of freedom/actuators exist. In terms of antiquity, Leonardo Da Vinci is believed to have created an iron man with an elaborate system of cable and pulley drives to move the arms and legs using a single water wheel [9]. In more recent times, tendon drives have been used to reduce the degrees of freedom of anthropomorphic finger mechanisms such as in the three-jointed two-degree-of-freedom finger [10] or the three-jointed single



Fig. 2 Potential use of a passive manipulation assist device based on the SDCSC configuration to form a “virtual reconfigurable manipulation guide-rail” in an industrial setting

degree-of-freedom finger [11]. Systematic methods of representing and analyzing the motion of complex cable-pulley mechanism configurations are discussed in detail in [8,12].

While past mechanisms may have been designed by trial and error or by using analysis, we will focus on determination of the dimensions of SDCSC mechanisms to satisfy a set of design specifications on end-effector motion by *synthesis*. Traditionally the kinematic synthesis of mechanisms to satisfy a desired set of specifications, is performed in two stages [13]. The first stage, *type synthesis*, involves the selection of a suitable type of mechanism for a particular task. Of specific interest is *number synthesis*, a subset of type synthesis, for determining the number of links and joints within a family of mechanisms to perform the desired task. In the second stage, *dimensional synthesis* methods are applied to determine the various dimensions, initial posture, and subsequent motion of the mechanism to match desired specifications. While both number and dimensional synthesis are critical steps, the determination of the appropriate number of links is often left to the discretion of the designer. In this paper, we will discuss development of tools to assist a designer accomplish both number and dimensional synthesis of SDCSC-type manipulators simultaneously.

From a mechanical-design standpoint, considerable attention has also focused on examining the harmonic-content of motions in the realm of linear vibrations [14,15]. The discrete Fourier transform has served as a convenient analysis tool within the design cycle of various types of flexible-structural-assemblies, ranging from hard-disk read heads [16] to flexible robotic mechanisms [17]. In recent years, several papers have also considered methods for suitably tailoring the harmonic content of mechanism-output motions over the entire motion cycle by design synthesis. Yuan and Rastegar [18,19] present systematic methods for optimum synthesis of four bars to eliminate selected ranges of high harmonics from the output-link motions for a constant angular-velocity input. Their method adjusts the nonlinear input–output relationship, introduced by the loop-closure constraints, by a suitably designing the full-cycle variation of the coupler-link length. This is then implemented using cam-follower mechanisms integrated at joints [18] or smart-materials integrated into the coupler link [19]. However, the focus in these papers is principally on function-generation synthesis to eliminate the mechanism-induced sources of vibrational excitement especially in high-speed systems.

In contrast, in this paper, we investigate the development of a synthesis scheme, leveraging tools from Fourier analysis and optimization, to permit the end effectors of SDCSC-configuration

manipulators to closely approximate desired closed planar paths. We note the seeming similarity of the proposed method to existing literature e.g. methods for synthesis of four-bar mechanisms for path generation using Fourier descriptors [20]. However, we will defer this discussion until Sec. 4, where we provide a detailed analysis and contrast of the proposed method in the context of existing literature in optimal-synthesis of path-following mechanisms.

3 Mathematical Preliminaries

Equations (1) and (2) represent the analysis and synthesis equations of the discrete Fourier transform (DFT) of a finite-length sequence of N data points of a uniformly sampled, periodic signal from the time domain, $x[j]$, to the frequency domain, $X[k]$. The set of harmonically related complex exponential sequences with frequencies that are integer multiples of $2\pi/N$ form a valid orthogonal basis for such periodic discrete signals. Linear combinations of these basis sequences can now be used to represent any data sequence that satisfies the Nyquist criterion and the discrete-time Dirichlet conditions [21] as:

$$X[k] = \text{DFT}[x[j]] = \sum_{j=1}^N x[j] e^{-i2\pi(k-1)(j-1)/N}, \quad 1 \leq k \leq N, \quad (1)$$

$$x[j] = \text{IDFT}[X[k]] = \frac{1}{N} \sum_{k=1}^N X[k] e^{i2\pi(j-1)(k-1)/N} \quad (1 \leq j \leq N). \quad (2)$$

Traditionally, the DFT has been used to extract the principal spectral components of signals where the N -point input data sequence, $x[j]$, is assumed to result from a *uniform sampling* of an N -term trigonometric series, with sampling rate F_s , as shown below:

$$\begin{aligned} x[j] &= a_0 + \sum_{k=1}^N a_k \cos(\omega_k t_j) + b_k \sin(\omega_k t_j) \\ &= A_0 + \sum_{k=1}^N A_k \cos(\psi_k + \omega_k t_j), \end{aligned} \quad (3)$$

$$\omega_k = \frac{2\pi(k-1)F_s}{N}, \quad t_j = (j-1) \frac{1}{F_s}, \quad 1 \leq j \leq N, \quad 1 \leq k \leq N.$$

By treating the discretely sampled sequence $x[j]$ as the input to the DFT algorithm, the unknown amplitudes, A_k , and phase-angles, ψ_k , corresponding to the N equally spaced, discrete frequencies, ω_k , may now be readily extracted from the DFT output, $X[k]$, as $a_0 = 2X[1]/N$, $a_k = 2 \text{Re}(X[k+1])/N$, $b_k = -2 \text{Im}(X[k+1])/N$, $A_k = \sqrt{a_k^2 + b_k^2}$, and $\psi_k = \arctan(b_k/a_k)$. These extracted parameters, can be used in conjunction with Eq. (3), to permit an *exact reconstruction* of the original sampled data-sequence, $x[j]$.

A few other relevant properties of the DFT are briefly summarized here for the reader's benefit. The DFT of two equal-length real-valued sequences can be computed simultaneously using complex-valued sequences, taking advantage of conjugate symmetry. Hence, all DFT operations are performed on complex-number sequences of desired end-effector positions, encoding both x and y coordinates of the desired path. Another noteworthy feature is that the total energy of the sequence before and after the DFT transformation is conserved, as shown in Eq. (4). This conservation principle, termed Parseval's Theorem, will be exploited to create an invariant energy-based objective function for the optimization problem developed in Sec. 4.

$$\sum_{j=1}^N [x[j]]^2 = \frac{1}{N} \sum_{k=1}^N [X[k]]^2. \quad (4)$$

4 Synthesis Methodology

A desired path-following task is presented as a set of prescribed end-effector positions to be matched or approximated as closely as possible by a SDCSC-configuration manipulator. Our interest is in the determination of such a manipulator with the smallest number of links, their dimensions and their initial configuration to perform this desired task.

4.1 Traditional Synthesis Approaches. Traditionally, the general mechanism design problem has been addressed within the framework of dimensional synthesis of mechanisms [13], the process of systematic selection of the (unknown) dimensions of this mechanism to match desired specifications. Within the overall dimensional-synthesis framework, optimization-based-synthesis and precision-point-synthesis (PPS) approaches have dominated and excellent review summaries may be found in [22,23].

PPS methods create constraints between mechanism parameters, by requiring an exact match of the end-effector positions at precision points. A simultaneous solution of the resulting set of nonlinear constraints then permits the determination of mechanism parameters. Optimization based synthesis methods use the minimization of an error objective function (such as the structural error) over the set of mechanism parameters to synthesize the mechanism. Other variants of synthesis methods, such as combining PPS with optimization in a constrained optimization scheme, also exist. One such approach was employed for the dimensional synthesis of SDCSC-based manipulators for planar [24] and spatial [25] rigid-body-guidance and path-following tasks.

Our work, in this paper, lies in the realm of continuous planar path following by the end effector (and for closed paths, in particular). However, for purposes of generality, we will assume that the continuous path may occasionally be specified to a designer, only as a set of discrete points (necessitating some form of interpolation). Optimal synthesis methods have been proposed for synthesis of linkages for such continuous paths following problems. However, these depend critically upon capturing the extent of the discrepancy between a desired and generated path specification. Traditionally, a "structural error," computed as the summed-squared-Euclidean distances between pairs of appropriately selected "correspondence points," has been employed as the "measure of discrepancy" of choice between the desired and generated curves. The overall problem is then formulated as a constrained minimization, using this structural error as the objective function subject to constraints to: guarantee the existence of a linkage solution; enforce dimensional-limits; and/or guarantee explicit satisfaction of the precision-position requirements for a subset of the path points in a combined PPS-optimization problem [13,24].

In motion generation problems, the desired end-effector orientation (or the inferred input-crank timing for a candidate-linkage solution) can help parameterize the set of desired end-effector positions and serve to ensure "correspondence." In contrast, in path-following problems, there is no correspondence between the generated path and the desired path due to the different parameterizations, except at the precision points (if any). Thus, determination of "correspondence" necessary for computation of the structural error has traditionally posed difficulties for path-following problems. Numerous methods for creating an artificial input-crank timing have been used, however, as several authors [20,26,27] note these have been more for ease of formulation within the structural-error-based optimization than for any practical relevance. It is also noteworthy that it is the determination of the structural error which is the ultimate goal. Zhou and Ting [27] also contain numerous references to other literature describing ways of creating a "suitable correspondence" using arc-length, nearest neighbors or cumulative bend-angle, thereby eliminating the dependence on an explicit specification of an (artificial) timing.

4.2 Proposed Fourier-Based Optimal Synthesis Approach. We will, however, explore the development of an alternative com-

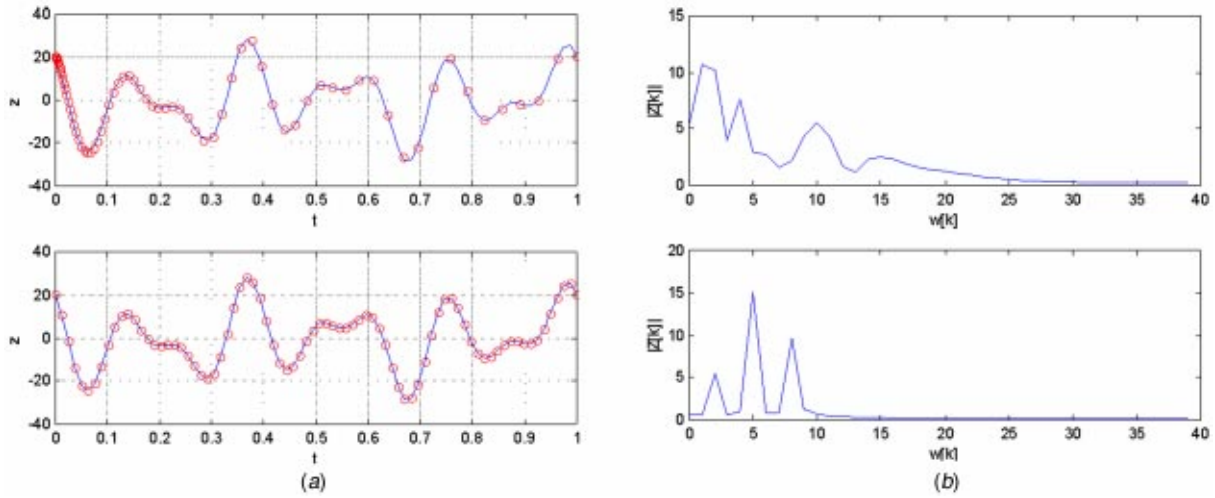


Fig. 3 (a) Geometric curve sampled with two different parameterizations (circles denote sampling locations); and (b) DFT transforms of the two sampled sets

putationally efficient method for synthesis of SDCSC-configuration manipulators for planar path following tasks, using tools from Fourier analysis and optimization. While closely allied to the traditional optimization-based mechanism-synthesis methods, our proposed method employs an *energy-based objective function* with the optimization being performed over a *set of non-mechanism parameters*, as elucidated later in this section.

Consider an n -link SDCSC mechanism with coupled joint rotations, created in a manner similar to the three-link mechanism shown in Fig. 1(a). The forward kinematics equations of this n -link SDCSC mechanism, at the j th position may be written in complex-number form as:

$$\mathbf{Z}_{P,j} = \mathbf{Z}_P(\phi_j) = \mathbf{Z}_0 + \mathbf{Z}_1 e^{i\phi_j} + \mathbf{Z}_2 e^{iR_1\phi_j} + \dots + \mathbf{Z}_n e^{iR_{(n-1)}\phi_j} \quad (5)$$

or equivalently, the two scalar equations may be written as:

$$\begin{aligned} x[j] &= x(\phi_j) = L_0 \cos(\Theta_0) + L_1 \cos(\Theta_1 + \phi_j) \\ &\quad + \dots + L_n \cos(\Theta_n + R_{(n-1)}\phi_j) \\ y[j] &= y(\phi_j) = L_0 \sin(\Theta_0) + L_1 \sin(\Theta_1 + \phi_j) \\ &\quad + \dots + L_n \sin(\Theta_n + R_{(n-1)}\phi_j), \end{aligned} \quad (6)$$

where, $L_k = \|\mathbf{Z}_k\|$ is the k th link length, $\Theta_k = \angle \mathbf{Z}_k$ is the k th link's initial orientation, R_i is the $(k+1)$ th absolute coupling ratio, $\theta_{1,j}$ is the absolute orientation of the 1st link at the j th position and ϕ_j is the relative input crank angle, i.e., the rotation of the 1st link relative to its initial orientation, Θ_1 . Specifically, we note that these forward kinematics equations take the special form of a finite trigonometric series, in terms of the input crank rotations, ϕ_j .

In a design scenario, the designer is usually presented with a set of M discrete path points along a given path, $z[m] = x[m] + iy[m]$, $\forall 1 \leq m \leq M$. An input crank parameterization $\phi[m]$ (in one-to-one correspondence with each data point, $z[m]$) is typically never provided in a path-following problem. This selection is left to the discretion of the designer, often without any specific guidelines. The sole constraint placed upon any such selected parameterization is that of monotonicity. Examples of parameterizations which could be used include: (a) a uniformly increasing sequence based on the normalized index of the data points in the

initial data sequence $z[m]$; (b) an increasing sequence based on the normalized path-length of each data point in the initial set $z[m]$; among others.

Hence, by selecting one such candidate parameterization $\phi[m]$, and using a cubic spline interpolation of the M data points, $z[m]$, one can create a set of N uniformly sampled data points, $z[j]$, $\forall 1 \leq j \leq N$. Using this uniformly sampled set, $z[j]$, as the sampled signal input to the DFT algorithm, the various amplitudes, A_k , frequencies, ω_k , and phase-angles, ψ_k , can now be extracted from the DFT output $Z[k]$. Our proposed mechanism synthesis scheme exploits the parallel between Eqs. (3) and (6) for determination of the mechanism parameters. We note that each of the extracted A_k , ω_k , and ψ_k have a ready and direct interpretation as the link lengths L_k coupling-ratios R_k and the initial link configurations Θ_k of the SDCSC mechanism which can trace the desired path, $z[j]$, and effectively constitutes the mechanism synthesis. This direct interpretation of the extracted Fourier coefficients is one distinguishing feature of our method compared to the Fourier-Descriptor based mechanism synthesis method [20].

4.2.1 Finite-Term Approximation. However, the synthesis method as outlined above suffers a major limitation in that all N terms of the DFT output, $Z[k]$, are required for an *exact* reconstruction of the input data sequence $z[j]$. With $N \approx 1024$, this would imply that an SDCSC mechanism with 1024 links would be needed to exactly reconstruct the original path. The redemption, however, comes from the fact that the greatest contribution to the reconstruction of the input data comes from the largest peaks in the DFT output. Hence, selecting a small number of the largest peaks ($n \ll N$), could still permit reconstruction of a *good approximation* of the input data. Physically, this would imply that an n -link SDCSC mechanism would be adequate to approximate the desired path. Hence, in our implementation, we further restrict the number of selected peaks, n , to be less than or equal to a designer-specified upper limit, $P \approx 5$.

4.2.2 Role of Input-Crank Angle Parameterization. At this stage, it is important to note that the parameterization of the input data plays a critical role in determining the number of significant terms in the DFT output. As an example, consider two sets of N discrete data points, obtained from the same one-dimensional geometric curve, by different sampling schemes. This process is depicted graphically in Fig. 3(a) with sampling locations denoted by circles. Both resulting data sets are then treated as uniformly sampled sequences and input to the DFT algorithm. The extracted

amplitudes A_k are plotted against the frequencies ω_k for both cases in Fig. 3(b). The DFT output for the first dataset shows *multiple significant peaks* with the implication that a multi-term trigonometric series would be required to reconstruct the original curve. In contrast, with a suitable parameterization (as in the second case) the DFT output clearly indicates that a three-term trigonometric series can well approximate the original geometric curve.

4.2.3 Input-Crank Angle Reparameterization. Thus, the proposed mechanism synthesis method is critically dependent upon the selection of a suitable input crank parameterization $\phi[m]$ for the initial data set, $z[m]$. To aid the designer in the suitable selection of $\phi[m]$, we create an initial input-crank angle parameterization, $\sigma[m]$, of the input data based on the normalized arc-length of the path to be traced. We then assume the existence of a polynomial functional mapping, $\pi: \sigma[m] \rightarrow \phi[m]$, which transforms this *initial guess* $\sigma[m]$ into the *desired* parameterization $\phi[m]$. An example of a such a polynomial functional mapping, a cubic, is shown below:

$$\phi[m] = A(\sigma[m])^3 + B(\sigma[m])^2 + C(\sigma[m]) + D \quad \forall 1 \leq m \leq M. \quad (7)$$

Suitable candidates for $\phi[m]$ can now be created by varying the polynomial coefficients (A , B , C , and D). The set of M data points, $z[m]$, with this parameterization $\phi[m]$ is interpolated using cubic splines, and used to generate a set of N uniformly sampled data points, $z[j]$, for input to the DFT algorithm. Candidate mechanism designs can now be generated by selecting P (or lesser) most significant peaks from the DFT output.

The end-effector of each candidate mechanism can now only trace the original path approximately. A quantitative measure of the degree of approximation may be obtained by considering the energy of the time- and frequency-domain sequences. By Parseval's theorem, the total energy of the time-domain sequence, $z[j]$, is preserved in the frequency-domain sequence, $Z[k]$. However, selecting only a finite number of peaks ($n \leq P \ll N$) from the frequency-data sequence, $Z[k]$, leads to the following inequality:

$$E_f \leq E_t \quad (8)$$

where

$$E_f = \frac{1}{N} \sum_{k=p}^N [Z[k]]^2 \quad \text{and} \quad E_t = \sum_{n=1}^N [z[j]]^2 = \frac{1}{N} \sum_{k=1}^N [Z[k]]^2,$$

where E_f reflects the energy captured by the P most significant peaks (indexed by \hat{p}) within the DFT output $Z[k]$ while E_t , reflects the energy of the entire time-domain data sequence $z[j]$.

4.2.4 Formulation of the Optimization Problem. If the selected mapping $\pi: \sigma[m] \rightarrow \phi[m]$ is incorrect, the DFT output would contain many significant peaks, and the energy content beneath a finite number of significant peaks would be much less than the total energy of the initial data. On the other hand, if a suitable mapping $\pi: \sigma[m] \rightarrow \phi[m]$ is found, a finite number of significant peaks in the DFT output would capture most of the energy of the original sequence. This forms the basis for the creation of our energy-based objective function, shown in Eq. (9). This further distinguishes the proposed method from the Fourier-descriptor based synthesis method reported in [20].

This search for an appropriate mapping $\pi: \sigma[m] \rightarrow \phi[m]$ may be posed in the form of an optimization problem as:

$$\text{Minimize}_{\pi: \sigma[m] \rightarrow \phi[m]} \left(1 - \frac{E_f}{E_t} \right) \quad (9)$$

where

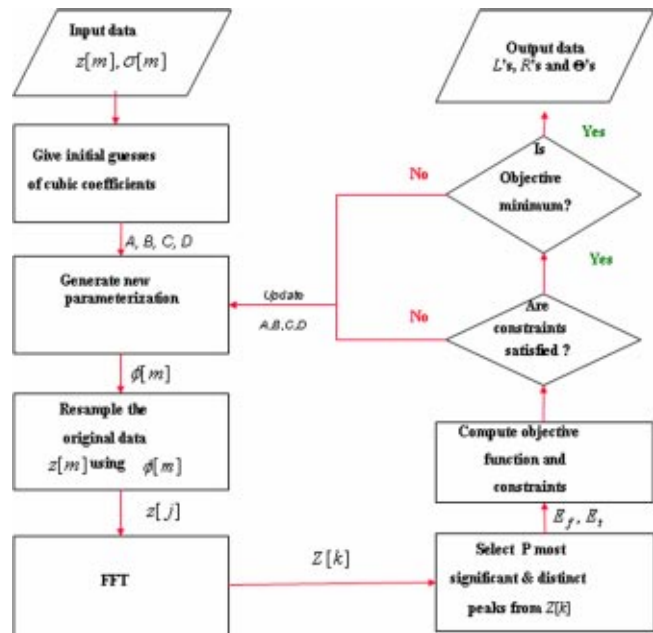


Fig. 4 Flowchart of the Fourier-based optimization

$$Z[k] = \text{DFT}[z[j]]$$

$$E_f = \frac{1}{N} \sum_{k=p}^N [Z[k]]^2, \quad E_t = \sum_{n=1}^N [z[j]]^2 = \frac{1}{N} \sum_{k=1}^N [Z[k]]^2$$

subject to,

$$\phi[m] \leq \phi[m+1] \quad \forall 1 \leq m \leq M-1.$$

Thus, the overall goal now becomes one of determining a suitable mapping, $\pi: \sigma[m] \rightarrow \phi[m]$, which minimizes the error in reconstruction of the input data by a finite trigonometric series with the smallest number of terms. In mechanism synthesis terms, this would then be equivalent to simultaneously performing number synthesis, to find an SDCSC mechanism with P links that can trace a desired path, and dimensional synthesis, to determine the values of the relevant link parameters.

Two additional criteria are employed for selecting distinct peaks in our implementation. First, an amplitude criterion is applied to discard peaks that are less than a minimum height to eliminate links that are too short. Second, a frequency-spacing criterion is used to create a minimum spacing between peaks. This is to prevent identical coupling ratios between adjacent links, in which case the two links could be replaced by a single rigid link. Other constraints, such as $\phi[m] \leq \phi[m+1] \quad \forall 1 \leq m \leq M-1$, are used to ensure monotonicity of the parameterization and prevent branching of the solution.

4.3 Software Implementation. This method was implemented in the form of a MATLAB-based software package. Figure 4 summarizes the overall implementation in the form of a flow chart. The optimization problem is solved using the *constr()* function in MATLAB's Optimization Toolbox, based on a sequential quadratic programming (SQP) method with Broydon-Fletcher-Goldfarb-Shanno Hessian updates at each iteration [28].

One distinguishing feature of this method is that the synthesis process can be completed in seconds, taking advantage of the speed of the signal processing algorithms, such as the FFT—the entire optimization process converges quickly, a few seconds on a Pentium™ II, 450 MHz computer running MATLAB 6. Furthermore, in contrast to traditional mechanism synthesis methods, all the parameters defining the optimal SDCSC mechanism (the link

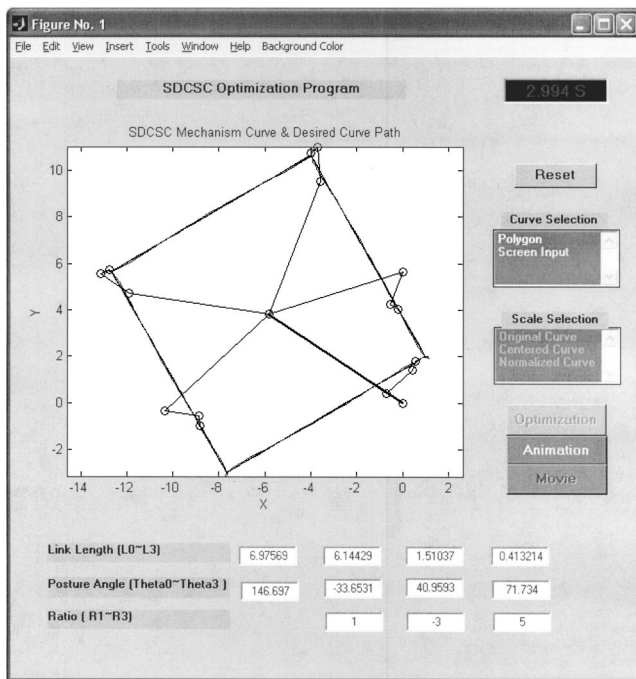


Fig. 5 GUI-based designer interface aids the designer in specifying and synthesizing SDCSC mechanisms (shown for a desired square end-effector path)

lengths, coupling ratios between every two adjacent joints and initial posture angles for each link) are determined simultaneously.

A Designer Interface was also developed and used to enhance the ability of the designer to interact with this synthesis in an intuitive manner with this software package using the Graphical User Interface (GUI) tools in MATLAB. The Designer Interface, shown in Fig. 5, permits the user to: (i) specify, save and manage the desired task specifications (as polygonal paths or by clicking on the screen from the user interface); (ii) display and animate multiple assembly configurations; and (iii) parametrically link to other CAD and control software to propagate the results of the synthesis.

5 Results

The selected task, representative of trajectories typically required in industrial applications, is to trace a $0.6 \text{ m} \times 0.3 \text{ m}$ rectangular path. This task combines straight-line traversals with sharp 90 deg bends which would traditionally pose problems for mechanism solutions. Three issues of interest arise, requiring decisions to be made by the designer.

First, SDCSC mechanisms with more links can be created by raising the upper limit on the number of peaks (P) in the Fourier-based optimization method. Such an increase creates SDCSC mechanisms capable of tracing more complex paths (using just one degree-of-freedom) at the cost of increased complexity of construction. Figure 6 depicts the incremental improvement of the matching when using two, three, four, and five links, respectively. However, we note that the last few links of the four- and five-link

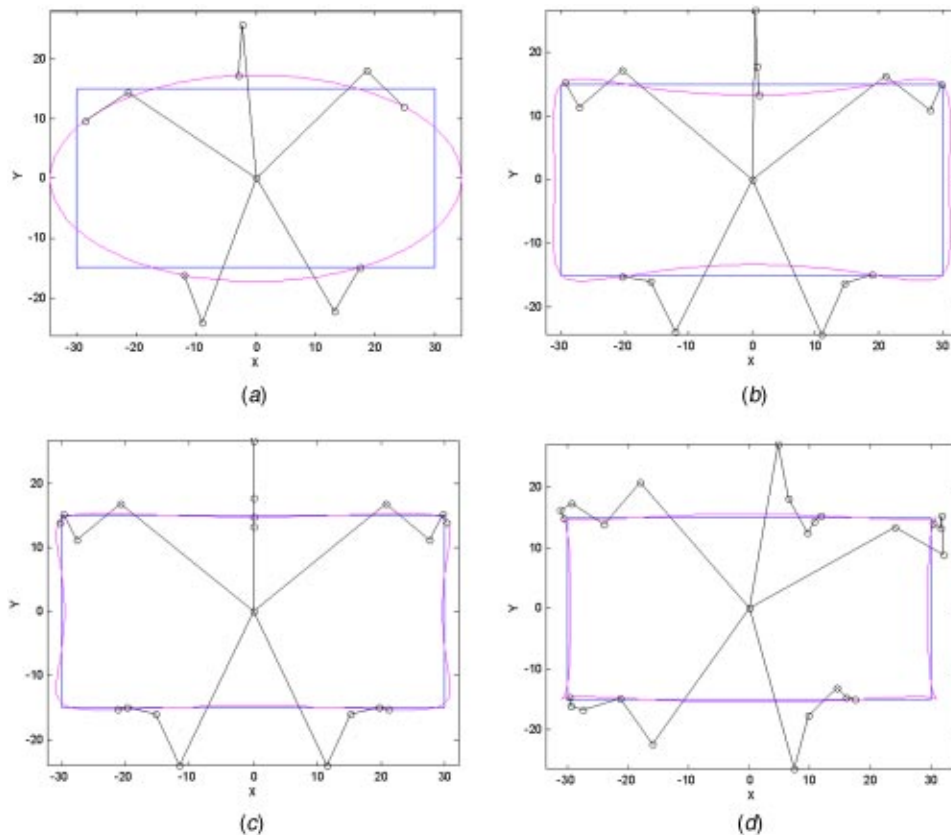


Fig. 6 Improved path tracing of a rectangular-path with increasing numbers of links: (a) two-link, (b) three-link, (c) four-link, and (d) five-link

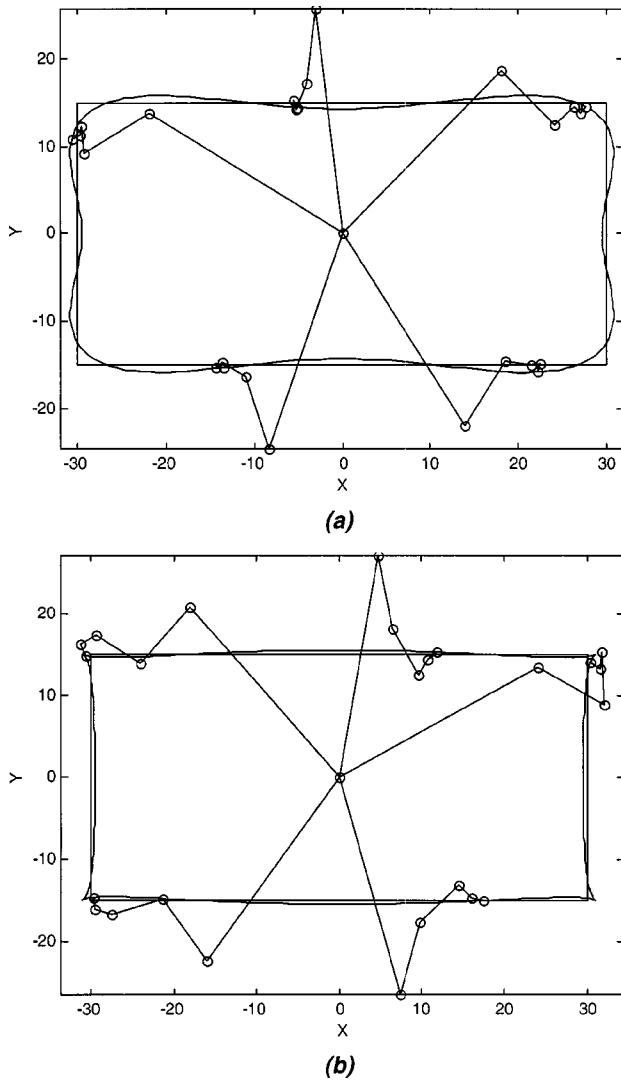


Fig. 7 Path tracing for a rectangular path (a) without and (b) with suitable dwell at corners

SDCSC mechanisms are very short, making them difficult to implement physically. Hence, in most cases, the designer would be required to specify small upper limits ($P < 5$) on the permissible number of links.

Second, the sharp corners of a desired path pose the greatest difficulty for matching with an SDCSC mechanism. Hence, when creating the *initial parameterization*, $\sigma[m]$, (in our case based on the normalized path length of the path to be traced) it is useful to create a dwell period at the sharp corners. This dwell period is created by repeatedly sampling the sharp corners in the initial data set $z[m]$, in a manner similar to the creation of “knots” for splines [29]. This has the effect of creating parametric continuity at the regions of reduced geometric continuity. This also mitigates the effects of abrupt changes in velocities during a sharp turn and improves matching at the corners, as seen in Fig. 7. Once again, the selection of this dwell in the initial parameterization is at the discretion of the designer.

Finally, we note that the greatest flexibility can be obtained by allowing the coupling ratio between any two joints to be a rational number. However, upon the successful synthesis for a single closed loop curve, the output for R_0 , coupling ratio for the first joint, is always 1, while the other ratios, from R_1 until R_{n-1} are integral multiples of the base coupling ratio as predicted by the

FFT implementation. This would appear to imply that the synthesis method limits us solely to realizing mechanism with integral coupling ratios. To overcome this seeming limitation, we include a pretreatment step, one of cyclic data point repetition, within the synthesis scheme. Given M data points on the original path, $z_1, z_2, \dots, z_{M-1}, z_M$, we concatenate multiple copies of the input data sequence to create multiple repeating cycles, as $\dots, z_1, z_2, \dots, z_{M-1}, z_M, z_1, z_2, \dots, z_{M-1}, z_M, \dots$. For Q concatenated copies of the input data points, the computed output for the fundamental frequency is scaled by a factor of Q . In renormalizing the computed frequency outputs by this factor, we see that the extracted coupling ratios can take on rational values. Thus, we note that intentionally repeating the given data points in additional cycles enhances the accuracy of computation of the coupling ratios (without requiring additional data).

6 Physical Design Process

For brevity, we restrict all further discussion in this section to the physical realization of an SDCSC mechanism with the smallest number of links to trace the given $0.60 \text{ m} \times 0.60 \text{ m}$ (24 in. \times 24 in.) square path. Fifty data-points were selected from each side of the square ($M=200$) and an initial arbitrary parameterization, $\sigma[m]$, was created based on the normalized arc length of the path. A cubic polynomial was used to create the desired parameterization $\phi[m]$ from this initial parameterization, by varying the coefficients. In every optimization iteration, the input data was interpolated with a candidate desired parameterization and sampled uniformly to create ($N=1024$) data points for input to the DFT algorithm. The optimization was performed with the end goal of designing a SDCSC mechanism with no more than three links ($P=3$). The relevant dimensions of the resulting three-link SDCSC mechanism, designed to trace the given square path are listed in Table 1.

Mathematically, the ordering of the terms in an m -term trigonometric series is not relevant. However, when considered as an n -link SDCSC mechanism, $m!$ physically different assembly configurations become possible based on the relative ordering of terms. Figure 8 depicts the six configurations of assembly of a three-link SDCSC mechanism with the same link-lengths, coupling ratios, and initial link-orientations. Each mechanism traces the same end-effector path but with a different overall link motions [4]. For example, the mechanisms shown in Fig. 8(c) and Fig. 8(e), stay entirely within the boundary of the generated path at all times, a useful feature in the presence of obstacles. The configurations shown in Figs. 8(a) and 8(d) are easy to construct, because the shortest link is the last link (and need not carry further belt-pulley couplings).

A physical prototype, shown in Fig. 9, was built based on configuration shown in Fig. 8(a), with successively decreasing link lengths. The emphasis was on creating a reconfigurable SDCSC-type manipulator to trace different sets of planar curves simply by altering the principal structural parameters. In particular, provision had to be made for the link-lengths to be varied continuously and for the coupling ratios to be varied continuously, over a reasonably wide design range.

The physical realization of a reconfigurable prototype while retaining the SDCSC configuration offered many challenges. Specifically, the links were designed modularly to permit changes in link lengths to permit easy reconfiguration to new tasks. Variable coupling ratios were achieved using continuously-variable-transmission (CVT) speed-reducers mounted on the base obtaining input from a common input shaft and subsequently the three output rotations of the speed reducers are transmitted to the corresponding joint using timing belts/pulleys. An innovative belt-tensioning idler design helped eliminate slack in the belts while allowing the center-center distances between the pulleys to be varied continuously using lead screws. The design was tested and analyzed in simulation prior to building physical prototype shown

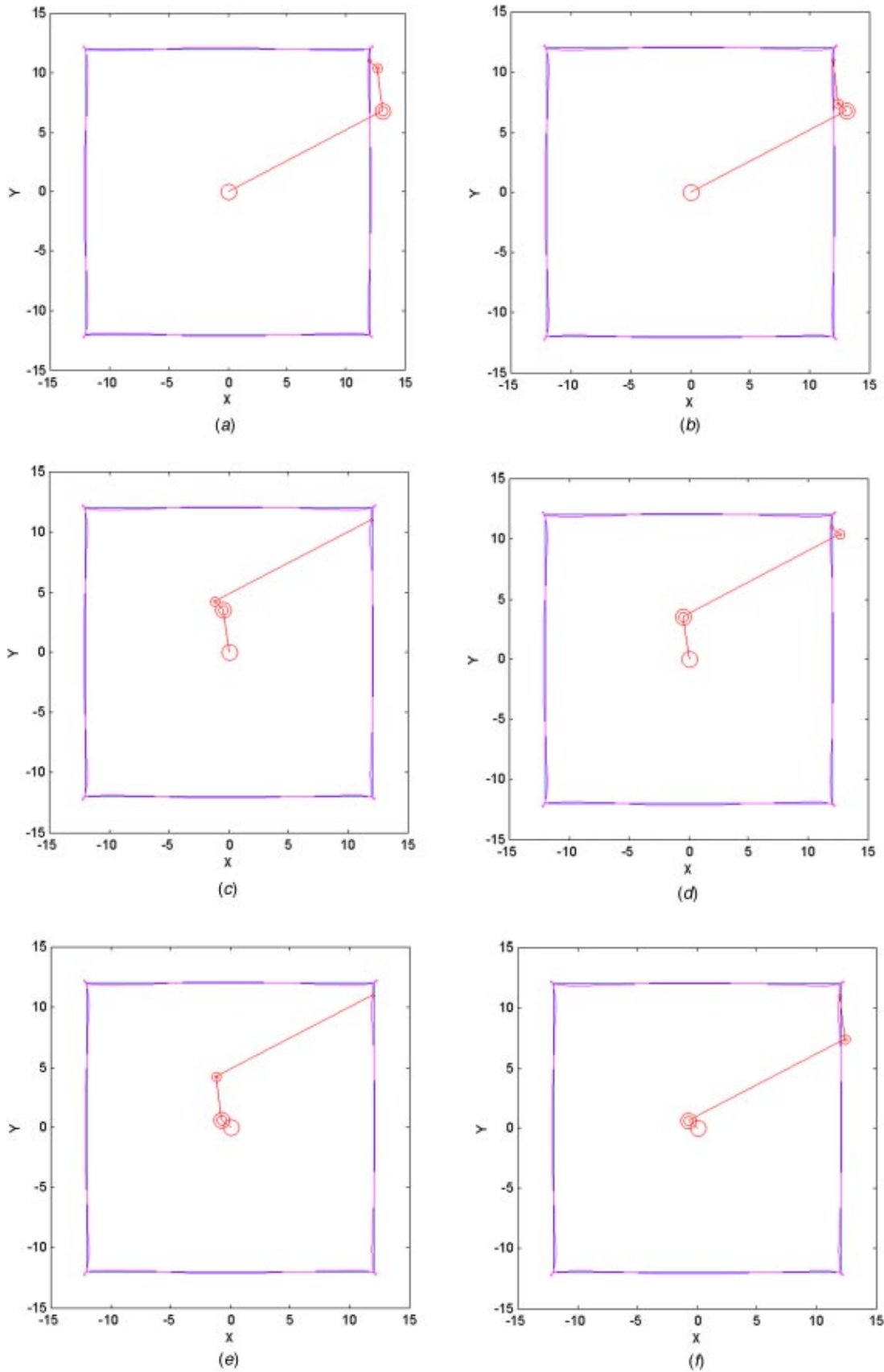
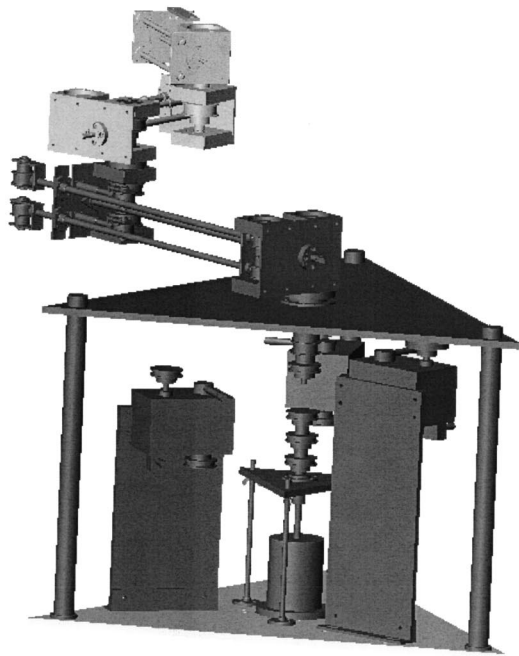


Fig. 8 Six assembly configurations of a three-link SDCSC mechanism synthesized by the Fourier-based synthesis method trace identical end-effector paths with different speeds



(a)



(b)

Fig. 9 Reconfigurable 3-link SDCSC mechanism: (a) parametric CAD model; and (b) fabricated physical prototype

Table 1 Dimensions of the optimal three-link SDCSC mechanism

$L_1 = 0.3753$ m (14.77 in.)	$R_0 = 1$	$\Theta_1 = 26.59$ deg (0.4641 rad)
$L_2 = 0.0941$ m (3.70 in.)	$R_1 = -3$	$\Theta_2 = 100.22$ deg (1.7493 rad)
$L_3 = 0.0275$ m (1.08 in.)	$R_2 = 5$	$\Theta_3 = 132.95$ deg (2.3205 rad)

in Fig. 9, which is currently undergoing further testing. The reader is referred to [4] for further details of the physical design and prototype implementation.

7 Conclusion

SDCSC-configuration based manipulators, with their single degree-of-freedom actuation and control and passive hardware constraint implementations, offer the potential to be flexible, low-cost alternatives to the more expensive, actively coordinated robotic manipulators for many of the typical industrial automation tasks. In this paper, we presented an alternative method for the kinematic synthesis of SDCSC-type manipulators for planar closed-loop path-following tasks, using techniques from Fourier analysis. The developed methods exploited the structure of the forward kinematic equations which take the form of a finite trigonometric series in terms of the input link rotation. A suitable input link rotation parameterization is critical to the mechanism design problem, but typically never provided for path-following tasks. The Fourier-based optimization method developed here assists designers with the process of determining a suitable input parameterization. The software implementation, together with the user-friendly designer interface, supports the designer in exploring various candidate SDCSC-configuration manipulator designs and to quickly determine *both* the number of links and the pertinent mechanism parameters. Furthermore, the availability of alternative assembly configurations of the optimal design was an added benefit. Overall, the results of this implementation show flexibility, reliability and repeatability.

Acknowledgments

The financial support of the Natural Sciences and Engineering Research Council (NSERC) of Canada and the Petro-Canada Young Innovator Award are gratefully acknowledged. We would also like to thank Yeow-Wei Pang for his early contributions [30] towards the creation of the design software.

References

- [1] Krovi, V., 1998, "Design and Virtual Prototyping of User-Customized Assistive Devices," Ph.D. thesis, Department of Mechanical Engineering and Applied Mechanics, University of Pennsylvania, Philadelphia, PA.
- [2] Hunt, K. H., 1978, *Kinematic Geometry of Mechanisms*, Clarendon Press, Oxford.
- [3] Nie, X., and Krovi, V., 2001, "Design of Passive Reconfigurable Manipulation Assistive Aids," DETC2001/DAC-21087, *Proceedings of the 2001 ASME Design Engineering Technical Conferences*, Pittsburgh, PA.
- [4] Nie, X., 2001, "Design of Reconfigurable Manipulation Assist Aids by Fourier Methods," M.Eng. thesis, Department of Mechanical Engineering, McGill University, Montreal, Canada.
- [5] Sandor, G. N., 1964, "On the Existence of a Cycloidal Burmester Theory in Planar Kinematics," *Trans. ASME*, 31, *J. Appl. Mech.*, **86**, pp. 694–699.
- [6] Wunderlich, W., 1970, "Chapter 33: Hoherer Radlinien," *Ebene Kinematik*, B.I-Hochschultaschenbuecher, No. 447/447A, Mannheim, Germany.
- [7] Kaufman, R. E., and Sandor, G. N., 1969, "Bicycloidal Crank: A New Four-Link Mechanism," *Trans. ASME, J. Eng. Ind.*, **91**, pp. 91–96.
- [8] Tsai, L.-W., 1995, "Design of Tendon-Driven Manipulators," *ASME J. Mech. Des.*, **117**, pp. 80–86.
- [9] Rosheim, M., 1997, "In the Footsteps of Leonardo," *IEEE Rob. Autom. Mag.*, **4**, pp. 12–14.
- [10] Leaver, S., McCarthy, J. M., and Bobrow, J., 1988, "The Design and Control of a Robot Finger for Tactile Sensing," *J. Rob. Syst.*, **5**, pp. 567–581.
- [11] Figliolini, G., and Ceccarelli, M., 1998, "A Motion Analysis for One D.O.F. Anthropomorphic Finger Mechanism," DETC98/MECH-5985, *Proceedings of the 1998 ASME Design Engineering Technical Conferences*, Atlanta, GA.
- [12] Hong, D. W., and Cipra, R. J., 2003, "A Method for Representing the Configuration and Analyzing the Motion of Complex Cable-Pulley Systems," *ASME J. Mech. Des.*, **125**, pp. 332–341.
- [13] Sandor, G. N., and Erdman, A. G., 1984, *Advanced Mechanism Design: Analysis and Synthesis*, Vol. 2, Prentice-Hall, Englewood Cliffs, NJ.

- [14] Rao, S. S., 2004, *Mechanical Vibrations*, 4th ed., Prentice-Hall, Upper Saddle River, NJ.
- [15] Thomson, W. T., and Dahleh, M. D., 1998, *Theory of Vibration With Applications*, 5th ed., Prentice-Hall, Upper Saddle River, NJ.
- [16] Lin, C.-C., 2002, "Finite Element Analysis of a Computer Hard Disk Drive Under Shock," *ASME J. Mech. Des.*, **124**, pp. 121–125.
- [17] Yu, S. D., and Xi, F., 2003, "Free Vibration Analysis of Planar Flexible Mechanisms," *ASME J. Mech. Des.*, **125**, pp. 764–772.
- [18] Yuan, L., and Rastegar, J., 2004, "Kinematics Synthesis of Linkage Mechanisms With Cam Integrated Joints for Controlled Harmonic Content of the Output Motion," *ASME J. Mech. Des.*, **126**, pp. 135–142.
- [19] Rastegar, J., and Yuan, L., 2002, "A Systematic Method for Kinematics Synthesis of High-Speed Mechanisms With Optimally Integrated Smart Materials," *ASME J. Mech. Des.*, **124**, pp. 14–20.
- [20] Ullah, I., and Kota, S., 1997, "Optimal Synthesis of Mechanisms for Path Generation Using Fourier Descriptors and Global Search Methods," *ASME J. Mech. Des.*, **119**, pp. 504–510.
- [21] Oppenheim, A. V., and Schaffer, R. W., 1992, *Discrete-Time Signal Processing*, Prentice Hall, Englewood Cliffs, NJ.
- [22] Angeles, J., and Liu, Z., 1993, in *Modern Kinematics: Developments in the Last Forty Years*, edited by A. G. Erdman, John Wiley & Sons, New York.
- [23] Chedmail, P., 1998, "Chapter I-5: Optimization of Multi-DOF Mechanisms," *Computational Methods in Mechanical Systems: Mechanism Analysis, Synthesis and Optimization*, Springer, Berlin.
- [24] Krovi, V., Ananthasuresh, G. K., and Kumar, V., 2002, "Kinematic and Kinostatic Synthesis of Planar Coupled Serial Chain Mechanisms," *ASME J. Mech. Des.*, **124**(2), pp. 301–312.
- [25] Krovi, V., Ananthasuresh, G. K., and Kumar, V., 2001, "Kinematic Synthesis of Spatial R-R Dyads for Path Following With Applications to Coupled Serial Chain Mechanisms," *ASME J. Mech. Des.*, **123**, pp. 359–366.
- [26] Zhou, H., and Cheung, H. M., 2001, "Optimal Synthesis of Crank-Rocker Linkages for Path Generation Using the Orientation Structural Error of the Fixed Link," *Mech. Mach. Theory*, **36**, pp. 973–982.
- [27] Zhou, H., and Ting, K.-L., 2002, "Adjustable Slider-Crank Linkages for Multiple Path Generation," *Mech. Mach. Theory*, **37**, pp. 499–509.
- [28] Vanderplaats, G. N., 1982, "Chapter 3: Unconstrained Optimization in N Variables," *Numerical Optimization Techniques in Engineering Design: With Applications*, McGraw-Hill, New York.
- [29] Farin, G., 1997, *Curves and Surfaces for Computer-Aided Geometric Design: A Practical Guide*, 4th ed., Academic Press, San Diego, CA.
- [30] Pang, Y.-W., 1999, "Fourier Methods for Synthesis of Coupled Serial Chain Mechanisms," Honors thesis, Department of Mechanical Engineering, McGill University, Montreal, Canada.